

## Formulation of structured bounding surface model with a destructuration law for natural soft clay

*Yunliang Cui, Xinquan Wang, Shiming Zhang*

Department of Civil Engineering, Zhejiang University City College,  
Hangzhou, China

*Received September 23, 2017*

A destructuration law considering both isotropic destructuration and frictional destructuration was suggested to simulate the loss of structure of natural soft clay during plastic straining. The term isotropic destructuration was used to address the reduction of the bounding surface, and frictional destructuration addresses the decrease of the critical state stress ratio as a reflection of reduction of internal friction angle. A structured bounding surface model was formulated by incorporating the proposed destructuration law into the framework of bounding surface constitutive model theory. The proposed model was validated on Osaka clay through undrained triaxial compression test and one-dimensional compression test. The influences of model parameters and bounding surface on the performance of the proposed model were also investigated. It is proved by the good agreement between predictions and experiments that the proposed model can well capture the structured behaviors of natural soft clay.

**Keywords:** natural soft clay; destructuration law; bounding surface; structured behavior

Для моделирования изменения структуры естественной мягкой глины при пластической деформации предложен метод деструктурирования с учетом изотропной деструктуры и фрикционной деструктуры. Структурная модель ограничивающей поверхности была сформулирована, применяя закон реструктурирования в рамках теории ограничивающих поверхностных конститутивных моделей. Предложенная модель была проверена на глине Осаки с помощью недренированного теста на трехосный компрессионный тест и одномерного теста на сжатие. Исследованы влияние параметров модели и ограничивающей поверхности на характеристики предложенной модели. Подтверждением хорошего согласования между прогнозами и экспериментами является то, что предлагаемая модель может хорошо фиксировать структурированное поведение естественной мягкой глины.

**Утворення моделі структурованої граничної поверхні відповідно до руйнування природної глини.** *Yunliang Cui, Changguang Qi, Xinquan Wang, Shiming Zhang.*

Для моделювання зміни структури природної м'якої глини при пластичній деформації запропоновано метод деструктування з урахуванням ізотропної деструктури і фрикційної деструктури. Структурна модель обмеженої поверхні була сформульована, застосовуючи закон реструктування в рамках теорії поверхневих конститутивних моделей. Запропонована модель була перевірена на глині Осаки за допомогою недренированого тесту на тривісний компресійний тест і одновимірного тесту на стиск. Досліджено вплив параметрів моделі і обмеженої поверхні на характеристики запропонованої моделі. Підтвердженням згоди між прогнозами і експериментами є те, що пропонується модель може добре фіксувати структувану поведінку природною м'якої глини.

### **I. Introduction**

Structure is common in natural soft clay, which is often defined as the fabric and bonding of soil particles. The progressive loss of soil structure during plastic straining is always

called “disturbance”[1], “degradation”[2] or “destructuration”[3]. The term destructuration is used in this paper to describe this kind of loss of structure. The destructuration leads to additional compression and strain softening of natural structured (or intact) clay which is

much different from the remoulded soil in stress-strain relationship. Experimental results[4, 5] indicate that the stress-strain relationship curve of natural clay has a softening after peak stress in triaxial compression with low confining pressure, and the compression rate of one-dimensional compression becomes faster when the compression pressure exceeds the structure yielding stress. It is well known that the well-established Modified Cam-Clay Model, which is based on remoulded soils, cannot capture the structured behaviors of natural soft clay. Some more advanced constitutive models[1, 2, 6] had been proposed to overcome this limitation. The pioneer introduction of bounding surface concept was initiated by Dafalias and Popov[7, 8] for metals' constitutive model. Dafalias[9] then extended and applied the bounding surface model to soils. Al-tabbaa and Wood[10] set a kinematic hardening yield surface, called 'bubble surface', inside the bounding surface to formulate a bubble model for soil. Based on the bubble model, Rouainia and Wood[11] presented a structured bounding surface model, using the structure surface as the bounding surface and incorporating a structure measure of the bounding surface. The structure measure allows the size of the bounding surface to decay with plastic straining, so that the proposed model can describe the loss of structure. With the similar method, Kavvadas and Amorosi[12] also proposed a model for structured soils which allows the external bond strength envelope (BSE) to shrink with the kinematic hardening of the internal plastic yield envelope (PYE). Some other researchers have done further research on such kind of structured bounding surface model and verified it with laboratory tests[13, 14]. Maranha and Vieira[15] implemented a "bubble" bounding surface model for structured soils, formulated by Kavvadas and Belokas[16] in finite element software FLAC to evaluate the influence of the initial plastic anisotropy in the excavation of a tunnel. Belokas and Kavvadas[17] also developed an incremental plasticity constitutive Model for Structured Soils to describe the effects of structured soils, such as high initial stiffness, dilatancy, peak strength and the evolution anisotropy. Overall, the various structured bounding surface models are based on the similar bounding surface framework, and mainly differ in the precise form of destructuration laws adopted. Therefore, it is of great importance to do research on destructuration law. It is seen in the above models that the destructuration laws only take the reduction of bounding surface into considered which can be defined as isotropic destructuration. However, some studies and experiments[3-5] show that natural structured clay has a higher internal friction angle than the corresponding remoulded clay. The friction angle of natural clay decreases

due to loss of structure. This is also demonstrated by the fact that the intact failure line lying above the post-rupture failure envelope. Because the critical state stress ratio is only related with the internal friction angle, the critical state stress ratio also decreases due to the reduction of friction angle. The frictional destructuration is defined to address the decrease of the critical state stress ratio as a reflection of reduction of internal friction angle. Taiebat et al.[3] suggested a destructuration law to address both isotropic and frictional destructuration and applied it on SANICLAY model. The frictional destructuration is proved to have significant effect on the loss of structure[3]. This study proposed a simple bounding surface model incorporating the destructuration law with some modifications. The proposed model can be seen as a simplified model of the existing structured bounding surface models[11-14], because it neglected some complex properties of soil, such as the kinematic hardening and anisotropy but considered the frictional destructuration. The performance of the proposed model is verified by typical experimental results on intact samples of natural soft clays.

## 2. Bounding surface model framework

### 2.1. General Elastic Stress-strain Relationship

It is the same as the Modified Cam-Clay model to calculate elastic stain with the following hypo-elastic stress-strain relationship:

$$\dot{\boldsymbol{\mu}}_{ij}^e = \mathbf{C}^e \cdot \boldsymbol{\Gamma}_{ij}^e \quad (1)$$

where  $\dot{\boldsymbol{\mu}}_{ij}^e$  is the incremental elastic strain,  $\boldsymbol{\Gamma}_{ij}^e$  is the incremental elastic stress, and  $\mathbf{C}^e$  is the elastic flexibility matrix. A dot ('·') operator denotes the matrix-vector and the matrix-matrix multiplications for clarity.  $\mathbf{C}^e$  can be written as

$$\mathbf{C}^e = \frac{1}{E} \begin{bmatrix} 1 & -\nu & -\nu \\ -\nu & 1 & -\nu \\ -\nu & -\nu & 1 \end{bmatrix} \quad (2)$$

where  $\nu$  is the Poisson's ratio and  $E$  is the elastic modulus which can be presented as  $E = 3p(1 - 2\nu)(1 + e_0) / \kappa$ . In this equation,  $e_0$  is the initial void ratio and  $\kappa$  is the slope of the swelling line in a volumetric strain-logarithmic mean stress plane.  $p$  is the mean effective stress, recalling that  $p = (\sigma_1 + \sigma_2 + \sigma_3) / 3$  in principal stress space.

### 2.2. Bounding Surface Function and Mapping Rule

It is considered for simplicity that the bounding surface has the same elliptical shape with the Modified Cam-Clay model.

$$F = \bar{p}^2 - p_c^* \bar{p} + \bar{q}^2 / M^{*2} \quad (3)$$

In Eq. (3),  $\bar{p}$  and  $\bar{q}$  are the mean effective stress and the generalized shear effective stress of the mapping point on the bounding surface of the current stress point, respectively.  $p_c^*$  is the intersection point of the bounding surface and the axial of  $p$ , which denotes the size of the bounding surface.  $M^*$  is the critical state stress ratio that is the slope of the critical state line. In this paper,  $p_c^*$  and  $M^*$  are the structure parameters related with plastic strain, which will be presented in detail later.

A radial mapping rule is adopted. The zero point in the stress space is taken as the mapping center. So the stress of the mapping point on the bounding surface is given by

$$\Gamma_{ij} = b\Gamma_{ij} \quad (4)$$

where  $b$  is the measure of the distance between the loading surface and the bounding surface, assuming that  $b = \delta_0 / (\delta_0 - \delta)$  and  $b \geq 1$ .

A schematic view of bounding surface model can be seen in Fig. 1.

According to the associated flow rule, the bounding surface is taken as the plastic potential surface, so the incremental plastic strain can be written as

$$\dot{\mu}_{ij}^p = \frac{1}{K_p} \left( \frac{\partial F}{\partial \Gamma_{kl}} \dot{\Gamma}_{kl} \right) \frac{\partial F}{\partial \Gamma_{ij}} = \frac{1}{K_p} \left( \frac{\partial F}{\partial \Gamma_{kl}} \Gamma_{kl} \right) \frac{\partial F}{\partial \Gamma_{ij}}$$

where  $\bar{K}_p$  is the plastic modulus at the mapping point on the bounding surface and  $K_p$  is the plastic modulus at the current stress point.

As is known,  $M$  is a constant and  $p_c$  is a hardening parameter in the Modified Cam-Clay model. This study changes  $M$  to  $M^*$  and  $p_c$  to  $p_c^*$  by means of adding destructuration factors which will be presented in detail in next section. The destructuration factors added to  $M$  and  $p_c$  involve plastic strains to form an evolution law.  $p_c^*$  and  $M^*$  will be both considered as internal variables in this model. Therefore, the consistency condition on the bounding surface should be written as

$$\frac{\partial F}{\partial \Gamma_{kl}} \dot{\Gamma}_{kl} + \frac{\partial F}{\partial P_c^*} \frac{\partial P_c^*}{\partial \mu_{ij}^p} \dot{\mu}_{ij}^p + \frac{\partial F}{\partial M^*} \frac{\partial M^*}{\partial \mu_{ij}^p} \dot{\mu}_{ij}^p = 0 \quad (6)$$

Substituting Eq. (5) into Eq. (6), the plastic modulus on the bounding surface is obtained by

$$\bar{K}_p = - \left( \frac{\partial F}{\partial P_c^*} \frac{\partial P_c^*}{\partial \mu_{ij}^p} \frac{\partial F}{\partial \Gamma_{ij}} + \frac{\partial F}{\partial M^*} \frac{\partial M^*}{\partial \mu_{ij}^p} \frac{\partial F}{\partial \Gamma_{ij}} \right) \quad (7)$$

The plastic modulus  $K_p$  can be obtained by interpolating according to the distance between the current stress point and the mapping point. On one hand, it is assumed that the interpolation modulus is zero when  $b = 1$ , that is to say  $K_p = \bar{K}_p$  when the current stress reaches

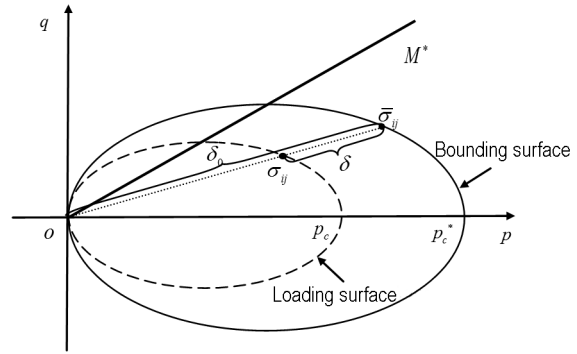


Fig. 1. Schematic view of bounding surface model.

the bounding surface. On the other hand, when the current stress point is very close to the zero stress point ( $b = \infty$ ), the plastic modulus  $K_p = \infty$ . Then it is possible to take a reasonable interpolation formula to obtain  $K_p$  at any current stress point. According to the proposal of Dafalias and Herrmann[9], the following interpolation formula is adopted:

$$K_p = \bar{K}_p + \zeta P_a \left( \left( \frac{\partial F}{\partial p} \right)^2 + \left( \frac{\partial F}{\partial q} \right)^2 \right) (b^\psi - 1) \quad (8)$$

where  $\zeta$  and  $\psi$  are interpolation parameters, reflecting the impact of the stress level on the modulus. Their values can be determined based on experimental curve fitting.

According to the associated flow rule, the plastic flexibility matrix can be presented as

$$C^p = \frac{\frac{\partial F}{\partial \Gamma_{ij}} \frac{\partial F}{\partial \Gamma_{kl}}}{K_p} \quad (9)$$

### 3. Formulation of structured bounding surface model

The basic framework of bounding surface model has been given above. In order to make the presented bounding surface model to consider the structure of soil, a reasonable structured hardening law will be introduced into the model. The hardening law used herein should combine hardening and softening. It is a common way to introduce a structure softening factor into the hardening parameter  $p_c$  to consider the destructuraion of the soil structure. This method allows the structured bounding surface to expand or shrink with plastic straining without changing of shape. This kind of destructuration is isotropic. However, there is a reduction of internal friction angle during the progressive loss of structure, reflected by the reduction of the critical state stress ratio, which is demonstrated by the bigger internal friction angle of the natural clay than that of the remoulded. It is named the frictinal destructuraion. In order

to consider the two kind of destructuration, two structured factors, that are isotropic destructuration factor  $S_i$  and frictional destructuration factor  $S_f$ , are incorporated in the proposed bounding surface model. A convenient approach is to revise  $p_c$  and  $M$  by  $S_i$  and  $S_f$ . Hence,  $p_c^*$  and  $M^*$  can be written as following:

$$p_c^* = S_i p_c \tag{10}$$

$$M^* = S_f M \tag{11}$$

where  $p_c$  contains a volumetric hardening rule controlled by the incremental plastic volumetric strain  $\dot{\epsilon}_v^p$  as the Modified Cam-Clay Model, which can be shown as

$$\dot{p}_c = p_c \frac{(1 + e_0)\dot{\epsilon}_v^p}{\lambda - \kappa} \tag{12}$$

$M$  is the critical state stress ratio which can be derived by  $M = 6 \sin \phi_c / (3 - \sin \phi_c)$ .  $\phi_c$  is the critical state internal friction angle of remoulded soil. Assuming that  $S_i$  and  $S_f$  are controlled by plastic strain,  $p_c^*$  and  $M^*$  can be rewritten in incremental form as following:

$$\dot{p}_c^* = \dot{S}_i p_c + S_i \dot{p}_c \tag{13}$$

$$\dot{M}^* = \dot{S}_f M \tag{14}$$

In Eq. (13),  $\dot{S}_i$  is assumed to be negative for softening while  $\dot{p}_c$  is positive for hardening, so  $S_i \dot{p}_c$  is the hardening part while  $\dot{S}_i p_c$  is the softening part. During the initial stage of the plastic straining, the size of bounding surface expands due to more hardening produced than softening. With more plastic strain occurring, the softening rate will become faster than hardening rate, leading to the shrinkage of the bounding surface. In Eq. (14),  $\dot{S}_f$  is also assumed to be negative due to the frictional destructuration, causing to the reduction of  $M^*$ . In this way, the critical state stress ratio of natural clay decreases progressively to be that of the remoulded soil with the loss of the structure. Thus an evolution equation for the  $S_i$  and  $S_f$  must be established. Taiebat et al.[3] has proposed an specific form of the evolution equation which reads

$$\dot{S}_i = -k_i \left( \frac{1 + e}{\lambda - \kappa} \right) (S_i - 1) \dot{\epsilon}_d^p \tag{15}$$

Table 1: Parameters of the model for Osaka clay

$\lambda$	$\kappa$	$v$	$M$	$S_{i0}$	$S_{f0}$	$m_i$	$m_f$	$\beta$	$\zeta$	$\psi$
0.154	0.02	0.25	1.279	6.9	1.102	1.2	1.2	0.5	18.0	0.5

$$\dot{S}_f = -k_f \left( \frac{1 + e}{\lambda - \kappa} \right) (S_f - 1) \dot{\epsilon}_d^p \tag{16}$$

As noted by Taiebat et al.[3], the above form is not the unique form for the evolution for the  $S_i$  and  $S_f$ , other forms can also be used. This study modified the above form and proposed an exponential form which reads

$$\dot{S}_i = - \frac{(S_i - 1)^{m_i}}{\lambda - \kappa} \dot{\epsilon}_d^p \tag{17}$$

$$\dot{S}_f = - \frac{(S_f - 1)^{m_f}}{\lambda - \kappa} \dot{\epsilon}_d^p \tag{18}$$

In Eq. (17) and Eq. (18),  $\lambda$  and  $\kappa$  are the slopes of the compression line and the swelling line in a volumetric strain-logarithmic mean stress plane, respectively. Both of  $m_i$  and  $m_f$  are material constants, which control the speed of the destructuration. The greater  $m_i$  and  $m_f$  are, the faster the destructuration are, therefore the faster the structured clay comes to the remoulded state. Since the main effect to be taken into account is the damage caused to the structure by both volumetric plastic strain  $\epsilon_v^p$  and deviatoric plastic strain  $\epsilon_q^p$ , the destructuration strain rate  $\dot{\epsilon}_d^p$ , which is a coupling internal variable, will be assumed to have the following form, as seen in literatures[11, 14].

$$\dot{\epsilon}_d^p = \sqrt{(1 - \beta)\dot{\epsilon}_v^{p2} + \beta\dot{\epsilon}_q^{p2}} \tag{19}$$

where  $\beta$  is a material constant distributing the effect of volumetric and deviatoric plastic strain rates to the value of  $\dot{\epsilon}_d^p$ .  $\beta$  could be set to 0.5 as a default value. The form of Eq. (19) suggests that for  $\beta = 0$  the destructuration is totally volumetric, while the destructuration is only controlled by deviatoric plastic strain when  $\beta = 1$ .

Substituting Eqs. (17), (18) and (19) into Eqs. (13) and (14), one can obtain the incremental expression of  $p_c^*$  and  $M^*$ . Substituting the destructuration laws Eqs. (12), (13) and (14) into Eq. (7), one can obtain  $\bar{K}_p$ , the plastic modulus at the bounding surface.

$$\begin{aligned} \bar{K}_p = & S_i \bar{p} \frac{(1 + e_0) p_c}{\lambda - \kappa} \frac{\partial F}{\partial \bar{p}} - \\ & - p_c \bar{p} \frac{(S_i - 1)^{m_i}}{\lambda - \kappa} \sqrt{(1 - \beta) \left( \frac{\partial F}{\partial \bar{p}} \right)^2 + \beta \left( \frac{\partial F}{\partial \bar{q}} \right)^2} - \end{aligned}$$

$$-\frac{2\bar{q}^2}{M^2 S_f^3} \frac{(S_f - 1)^{m_f}}{\lambda - \kappa} \sqrt{(1-\beta) \left(\frac{\partial F}{\partial p}\right)^2 + \beta \left(\frac{\partial F}{\partial q}\right)^2} \quad (20)$$

The plastic modulus at the current stress point, that is  $K_p$ , can be derived by substituting Eq. (20) into Eq. (8). Therefore, the plastic flexibility matrix  $C^p$  can be obtained by Eq. (9).

#### 4. Parameters determination and model verification

Parameters of the proposed model can be determined in following ways: To begin with,  $\lambda$ ,  $\kappa$  and the initial isotropic structure parameter  $S_{i0}$  are determined by one-dimensional compression test. Critical state stress ratio  $M$ , Poisson's ratio  $\nu$  and initial frictional structure parameter  $S_{f0}$  are determined by triaxial compression test. Then, the adaptive parameter  $\mu$  is determined by true triaxial test. Finally, the material constants  $m_i$ ,  $m_f$ ,  $\zeta$  and  $\psi$  are determined by fitting the stress-strain curve of triaxial compression.

For Osaka Clay[4], the values of parameters  $\lambda$ ,  $\kappa$  were obtained from an isotropic consolidation test[4], which gives  $\lambda = 0.355/2.303 = 0.154$ ,  $\kappa = 0.0477/2.303 = 0.02$ .  $S_{i0}$  and  $S_{f0}$  are used to denote the initial value of  $S_i$  and  $S_f$ , respectively, which reflect the initial degree of the structure of natural soil.  $S_{i0}$  can be determined by one-dimensional compression tests on natural soil and the corresponding remoulded soil. Its value is equal to the ratio of  $p_y$  to  $p_0$  where  $p_y$  is the structure yielding pressure on the compression line of natural soil and  $p_0$  is the pressure on the compression line of the remoulded soil corresponding to the same void ratio with  $p_y$ . The concept of structure yielding pressure  $p_y$  is based on the assumption that structure begins to loose when compression pressure exceeds  $p_y$  and no structure loss occurs if compression pressure is less than  $p_y$ . As seen in Figure 5, the value of  $S_{i0}$  for Osaka clay is determined by  $S_{i0} = p_y / p_0 = 94.1/13.7 = 6.9$ .  $S_{f0}$  can be determined by triaxial compression tests on natural soil and the corresponding remoulded soil. Its value is equal to the ratio of  $M^*$  to  $M$ .  $M^*$  and  $M$  are the critical state stress ratios of natural soil and the remoulded soil, respectively. As shown in reference[4],  $M^* = 1.41$ , effective internal frictional angle of remoulded soil  $\phi = 31.8^\circ$ .

. Then  $M = \frac{6 \sin \phi}{3 - \sin \phi} = 1.279$ , and the value of  $S_{f0}$  for Osaka clay is determined by  $S_{f0} = M^* / M = 1.102$ . The adaptive parameter  $\mu$  can be derived by comparing the predictions of the adaptive criterion with the experimental results from true triaxial test.  $m_i$  and  $m_f$  are

used to control the isotropic destructuration rate and the frictional destructuration rate, respectively. Given that the isotropic destructuration and the frictional destructuration proceed at the same rate, their values can be assumed to be the same. The values of  $m_i$  and  $m_f$  for Osaka clay is determined to be  $m_i = m_f = 1.2$  by fitting the stress-strain curve of triaxial compression test.  $\beta$  controls the relative contributions of  $\dot{\epsilon}_v^p$  and  $\dot{\epsilon}_q^p$  to the incremental destructuraion plastic strain  $\dot{\epsilon}_d^p$ , so its value can be determined as  $\beta = 0.5$  in default before further study.  $\zeta$  and  $\psi$  are used for modulus interpolation between the bounding surface and the current stress point. Their values can be determined by fitting the stress-strain curve of triaxial compression. In this way, the values of  $\zeta$  and  $\psi$  for Osaka clay are determined as  $\zeta = 18.0$  and  $\psi = 0.5$ .

The triaxial compression test performed on sample TS5-2 of Osaka clay[4] is used herein to verify the model's capabilities. In this test, the sample was compressed under undrained condition after isotropic consolidation. The initial stress state is  $\sigma_1 = \sigma_2 = \sigma_3 = 78.4$  kPa, The initial void ratio of the specimen is  $e_0 = 1.9$ . The optimized parameters used in these simulations are listed in Table 1. These optimized parameters are described as the reference parameters. Figure 2 gives the simulation stress-strain curve and the test stress-strain curve of the consolidated undrained triaxial compression test. Figure 3 shows the comparison of the simulation stress path and the test stress path. A good agreement of simulation curves with experimental curves can be seen in Figure 2 and Figure 3. This demonstrates that the proposed model is capable of modeling the peak strength and strain softening of natural soft clay under the condition of consolidated undrained triaxial compression.

The best way to validate the capabilities of the model is to validate it with a parameters-independent test. Parameters-independent test refers to a set of tests which have not been used to determine parameters. As a parameters-independent test, test TS5-3[4] is simulated by taking the same parameters with test TS5-2. Test TS5-3 was also performed with consolidated undrained triaxial compression. The consolidation stress is  $\sigma_1 = \sigma_2 = \sigma_3 = 39.2$  kPa, which is much lower than that of test TS5-2. The comparisons of predictions and experiments of TS5-3 can be seen in Figure 3 and Figure 4. As shown in Figure 3 and Figure 4, the predictions and experiments of test TS5-3 show worse agreement compared with test TS5-2. However, the agreement is good enough for engineering calculations. Modified Cam-clay model was also used to simulate test TS5-3 to be compared with the structured bounding surface model in this work. The parameters

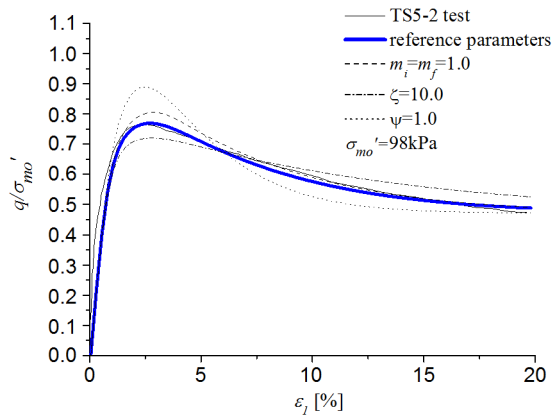


Fig. 2. Comparisons of prediction and experimental stress-strain curves of test TS5-2.

of Modified Cam-clay model  $\lambda$ ,  $\kappa$ ,  $\nu$  and  $M$  have the same values with the proposed model, which are shown in Table 1. As seen in Figure 4, the comparisons indicate that Modified Cam-clay model is not able to predict the experimental stress-strain curve and the proposed model can give a better agreement. Modified Cam-clay model predicts a much lower strength due to neglecting the structure of soil.

A general indication of the influences of the fitting parameters on the response in the test is also shown in Figure 2. Such a study provides assistance in the search for the optimized parameters to match experimental observations. The consequences can be summarized as follows: Reducing  $m_i$  and  $m_f$  reduces the rate of destructuration, and hence raises the peak strength because destructuration occurs more slowly. Reducing  $\zeta$  reduces the plastic modulus and hence smoothes the peak.  $\psi$  has the similar influence with  $\zeta$ . Increasing  $\psi$  leads to a higher and sharper peak of the stress-strain relationship.

The oedometer test was performed to get the one-dimensional compression results. The initial void ratio of the specimen is  $e_0 = 1.9$ . It was first consolidated by vertical pressure  $\sigma'_v = 4.9 \text{ kPa}$  to be at the state of  $e = 1.8$ , and then loaded stage by stage. The model parameters are the same with those of the triaxial compression test, which are shown in Table 1. Figure 5 shows the comparison between the simulation curve and the experimental curve. It can be seen that the proposed model can well capture the structured characteristics that the compression of natural clay become faster when the pressure exceed the structure yield stress.

This work introduces the destructuration law into a bounding surface model instead of a simple yield surface model, although the bounding surface theory makes the model complex. In order to show the importance of using the bounding surface, this study repeats some

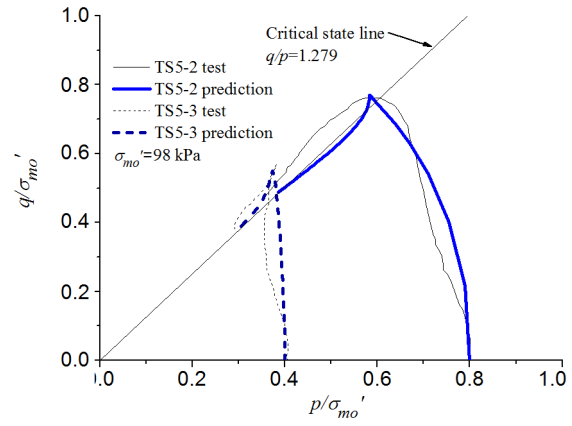


Fig. 3. Comparisons of prediction and experimental stress paths of Osaka clay.

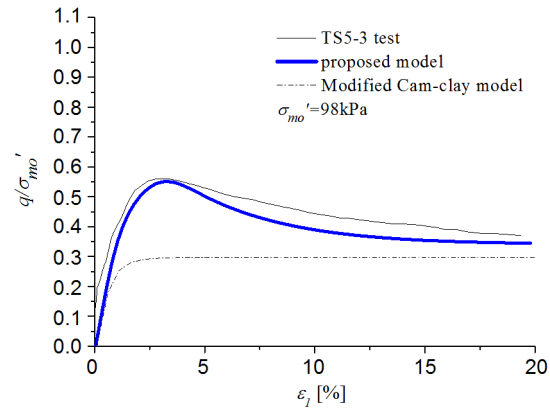


Fig. 4. Comparisons of prediction and experimental stress-strain curves of test TS5-3.

simulations of undrained triaxial compression tests of Osaka clay without the use of bounding surface and compares the new simulations with the one with the bounding surface. The change of bounding surface model to a regular yield surface model is done by modifying the formula of plastic modulus which uses bounding surface as yield surface, namely,  $b = 1$  in Eq. (8). As seen in Figure 6, the comparisons show that the simulations with bounding surface are much better than the ones without bounding surface. Thus, from a practical perspective, using the bounding surface in the proposed model is important. Besides, the use of bounding surface brings the advantage of simulating cyclic loading which cannot be properly done by the model with regular yield surface. This is also one of the reasons to use bounding surface in this work, which will be discussed more in further study.

#### 4. Conclusions

Both isotropic destructuration and frictional destructuration of natural clay can be considered by adopting the suggested destructuration law in bounding surface constitutive model.

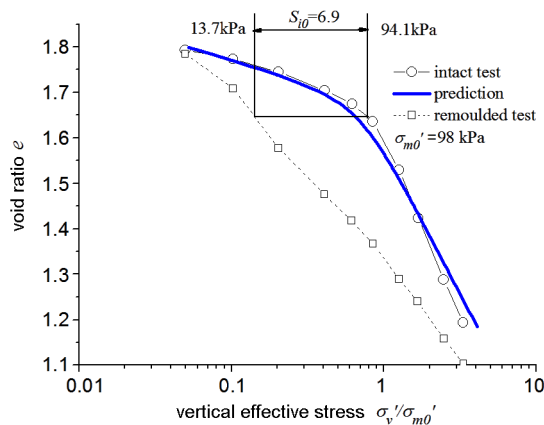


Fig. 5. Comparisons of prediction and experimental stress-strain curves of test TS5-3.

Isotropic destructuration was used to address the reduction of the bounding surface, and frictional destructuration addresses the decrease of the critical state stress ratio as a reflection of reduction of internal friction angle. The Isotropic destructuration and frictional destructuration laws were proposed by incorporating isotropic destructuration factor  $S_i$  and frictional destructuration factor  $S_f$  to revise isotropic hardening parameter  $p_c$  and critical state stress ratio  $M$ . The evolution law for the  $S_i$  and  $S_f$  has an exponential form.

By simulating undrained triaxial test and one dimensional compression test on Osaka clay, it is proved that the formulated bounding surface model in this study can well capture the structured behaviors of natural soft clay. This model is capable of modeling the peak strength and strain softening of natural soft clay under the condition of consolidated undrained triaxial compression, and it can well reflect the structured characteristics that the compression of natural clay become faster when the pressure exceed the structure yield stress.

This bounding surface model can be changed to be a regular yield surface model by modifying the formula of plastic modulus. However, the simulations of experiments of the model with bounding surface are much better than the ones without bounding surface.

**Acknowledgment** The support of Zhejiang Provincial Natural Science Foundation of China (Grant no. LQ16E080007), National Natural Science Foundation of China (Grant no. 51508507) and Zhejiang Provincial Educational Scientific Research project (Grant no. Y201533738) are gratefully acknowledged.

### References

1. C. S. Desai, *J. GeoMech.*, **7**, 83, 2007. doi: 10.1061/(ASCE)1532-3641(2007)7:2(83).

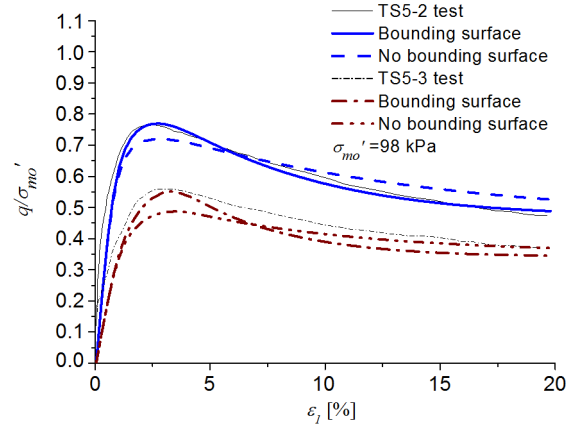


Fig. 6. Comparison of predictions with and without bounding surface.

2. C. Hu, H. Liu, W. Huang, *Comp. Geotechn.*, **44**, 34, 2012. doi: 10.1016/j.compgeo.2012.03.009.
3. M. Taiebat, Y. F. Dafalias and R. Peek, *Int. J. Num. Anal. Meth. Geomech.*, **34**, 1009, 2010, doi: 10.1002/nag.841.
4. T. Adachi, F. Oka, T. Hirata, T. Hashimoto, J. Nagaya, M. Mimura and TBS. Pradhan, *Soils Found.*, **35**, 1, 1995.
5. L. Callisto and G. Calabresi, *Geotechn.*, **48**, 495, 1998.
6. H. S. Yu, *Int. J. Num. Anal. Meth. Geomech.*, **22**, 621, 1998. doi: 10.1002/(SICI)1096-853(199808)22:8<621::AIDNAG937>3.0.CO;2-8.
7. Y. F. Dafalias, E. P. Popov, *Acta Mech.*, **21**, 173, 1975.
8. Y. F. Dafalias, E. P. Popov, "Plastic Internal Variables Formalism of Cyclic Plasticity," American Society of Mechanical Engineers, 1976.
9. Y. F. Dafalias, L. R. Herrmann, *J. Eng. Mech.*, **112**, 1263, 1986.
10. A. Al-Tabbaa, D. M. Wood, *Proceeding of the 3rd International Conference on Numerical Models in Geomechanics*, 1989, pp.91-99.
11. M. Rouainia, D. M. Wood, *Geotechn.*, **50**, 153, 2000.
12. M. Kavvas, A. Amorosi, *Geotechn.*, **50**, 263, 2000.
13. L. Callisto, A. Gajo, D. M. Wood, *Geotechn.*, **52**, 649, 2002. doi: 10.1680/geot.52.9.649.38840.
14. A. Gajo, D. M. Wood *Int. J. Num. Anal. Meth. Geomech.*, **25**, 207, 2001. doi: 10.1002/nag.126.
15. J. R. Maranhã, A. Vieira, *Acta Geotech.*, **3**, 259, 2008.
16. M. Kavvas and G. Belokas, "An Anisotropic Elastoplastic Constitutive Model for Natural Soils," Desai et al. (eds) *Computer methods and advances in geomechanics*, Balkema Rotterdam, 2001, pp.335-340.
17. G. Belokas, M. Kavvas, *Comp. Geotechn.*, **37**, 737, 2010, doi: 10.1016/j.compgeo.2010.05.001.